Tellus (1997), 49B, 18–37
Printed in UK – all rights reserved

TELLUS
ISSN 0280–6509

Linking a global terrestrial biogeochemical model and a 2-dimensional climate model: implications for the global carbon budget

By X. XIAO[1,2]*, D. W. KICKLIGHTER[1], J. M. MELILLO[1], A. D. McGUIRE[1,3], P. H. STONE[2] and A. P. SOKOLOV[2], [1]*The Ecosystems Center, Marine Biological Laboratory, Woods Hole, MA 02543, USA;* [2]*The Joint Program on the Science and Policy of Global Change, Massachusetts Institute of Technology, Cambridge, MA 02139, USA;* [3]*National Biological Service, Alaska Cooperative Fish and Wildlife Research Unit, University of Alaska, Fairbanks, AK 99775, USA*

(Manuscript received 20 September 1995; in final form 6 June 1996)

ABSTRACT

We used the terrestrial ecosystem model (TEM, version 4.0) to estimate global responses of annual net primary production (NPP) and total carbon storage to changes in climate and atmospheric CO_2, driven by the climate outputs from the 2-dimensional MIT L-O climate model and the 3-dimensional GISS and GFDL-q atmospheric general circulation models (GCMs). For contemporary climate with 315 ppmv CO_2, TEM estimates that global NPP is 47.9 PgC/yr and global total carbon storage is 1658 PgC: 908 PgC of vegetation carbon and 750 PgC of reactive soil organic carbon. For climate change associated with a doubling of radiative forcing and an atmospheric level of 522 ppmv CO_2, the responses of global NPP are +17.8% for the MIT L-O climate, +18.5% for the GFDL-q climate and +20.6% for the GISS climate. The responses of global total carbon storage are +6.9% for the MIT L-O climate, +8.3% for GFDL-q climate and +8.7% for the GISS climate. Among the three climate change predictions, the changes in latitudinal distributions of cumulative NPP and total carbon storage along 0.5° latitudinal bands vary slightly, except in high latitudes. There are generally minor differences in cumulative NPP and total carbon storage for most of the 18 biomes, except for the responses of total carbon storage in boreal biomes for the 2-D MIT L-O climate change. The results demonstrate that the linkage between the TEM and the 2-D climate model is useful for impact assessment and uncertainty analysis within an integrated assessment framework at the scales of the globe, economic regions and biomes, given the compromise between computational efficiency in the 2-D climate model and more detailed spatial representation of climate fields in 3-D GCMs.

1. Introduction

Atmospheric CO_2 concentration has increased since the pre-industrial era from about 280 ppmv to 356 ppmv (IPCC, 1994, 1995). The average rate of CO_2 concentration increase during the 1980s was 0.4% or 1.5 ppmv per year, which is equivalent to 3.2 PgC/yr, approximately 50% of total anthropogenic CO_2 emission (IPCC, 1994, 1995). There are large uncertainties about the path and magnitude of future anthropogenic emission of greenhouse gases, because of uncertainty in population growth, economic growth, technology development and other factors. These uncertainties, combined with uncertainties in natural biogeochemical cycles, lead to questions about the rate and magnitude of changes of concentrations of greenhouse gases (especially CO_2) in the atmosphere.

* Corresponding author.
email: xiao@lupine.mbl.edu

Increases in CO_2 and other greenhouse gases in the atmosphere will increase the radiative forcing of climate. The resultant climate change combined with the increase of atmospheric CO_2 concentration may in turn have significant impacts on the structure and biogeochemistry of terrestrial ecosystems (Gates, 1985; Houghton and Woodwell, 1989; Melillo et al., 1990; Jenkinson et al., 1991). At the global and continental scales, a number of studies have investigated the potential impact of climate change and elevated CO_2 on primary production and carbon storage of natural ecosystems and managed ecosystems. One approach has applied $+1°C$, $+2°C$ or $+4°C$ temperature increase and/or $\pm 10\%$, $\pm 20\%$ change of precipitation uniformly over a study area (Esser, 1987, 1990; Buol et al., 1990; Zhang, 1993; Potter et al., 1993; McGuire et al., 1993, 1995; Schimel et al., 1994; Melillo et al., 1995). This simple approach ignores potential differences in both latitudinal and longitudinal variations in temperature and precipitation. Another approach uses climate outputs from 3-dimensional atmospheric general circulation models (3-D GCMs) for doubled CO_2 scenarios (Melillo et al., 1993; VEMAP Members, 1995; Parton et al., 1995; Rosenzweig and Parry, 1994). Outputs from these 3-D GCMs are commonly used: Goddard Institute for Space Studies (GISS ; Hansen et al., 1983, 1984), Geophysical Fluid Dynamic Laboratory (GFDL; Manabe and Wetherald, 1987; Wetherald and Manabe, 1988), Oregon State University (OSU, Schlesinger and Zhao, 1989), and United Kingdom Meteorological Office (UKMO, Wilson and Mitchell, 1987). These climate outputs represent equilibrium climate for doubled concentrations of atmospheric CO_2.

A significant number of climate change simulations (including transient climate change) associated with different scenarios of anthropogenic emissions of greenhouse gases need to be explored in order to quantify uncertainties and impacts of global climate change that are relevant to policy and decision making (Jacoby and Prinn, 1994). Because 3-D GCMs require substantial computational resources, the application of 3-D GCMs in uncertainty analysis and impact assessment of climate change is at present limited. By observing that latitudinal variations play a stronger role than longitudinal variations in determining climate, and that transport by large-scale 3-D eddies can be parameterized by using dynamical theory, a 2-dimensional climate model has been used to study climate change (Land-Ocean climate model, namely as 2-D MIT L-O climate model, see Yao and Stone, 1987; Stone and Yao, 1987, 1990; Sokolov and Stone, 1995). The 2-D MIT L-O climate model simulates the zonally averaged climate separately over land and ocean as a function of latitude and height. The 2-D model runs 23 times faster than the GISS GCM with $8°$ (latitude) $\times 10°$ (longitude) resolution and 115 times faster than the GISS GCM with $4° \times 5°$ resolution. The 2-D model takes a few days for an equilibrium simulation and is capable of simulating many more long-term (100–150 years) transient climate change scenarios within a reasonable time than a 3-D GCM, therefore it is potentially very useful for uncertainty analysis and impact analysis at large spatial scales, e.g., the globe.

The 2-D L-O climate model is at the heart of the integrated assessment framework for climate change at the Massachusetts Institute of Technology (MIT), which includes a set of coupled models and is shown schematically in Fig. 1. Human activity leads to emissions of chemically and radiatively important trace gases. The combined anthropogenic and natural emissions are the driving forces for the coupled atmospheric chemistry and the 2-D L-O climate model. The climate model outputs drive a terrestrial ecosystem model that predicts terrestrial biogeochemical cycles, including land CO_2 fluxes. The outputs from the terrestrial ecosystem model feed back to the climate model, atmospheric chemistry model, natural emissions model and economic model. The coupling of the Terrestrial Ecosystem Model (TEM) in the framework allows us to study the role of biogeochemistry in the context of interactions among climate, biology and economics.

In this study, we use a new version of the Terrestrial Ecosystem Model (McGuire et al., 1995), driven by climate outputs from two 3-D GCMs and the 2-D MIT L-O climate model. Our objective is to compare the ecological consequences of climate changes as simulated by the 2-D climate model and 3-D GCMs. We are primarily interested in the impacts of climate change at highly aggregated spatial scales (globe, latitudinal bands, economic regions and biomes). Thus, we examine the similarities and differences in the responses of NPP and total carbon storage to different climate change predictions from the 2-D

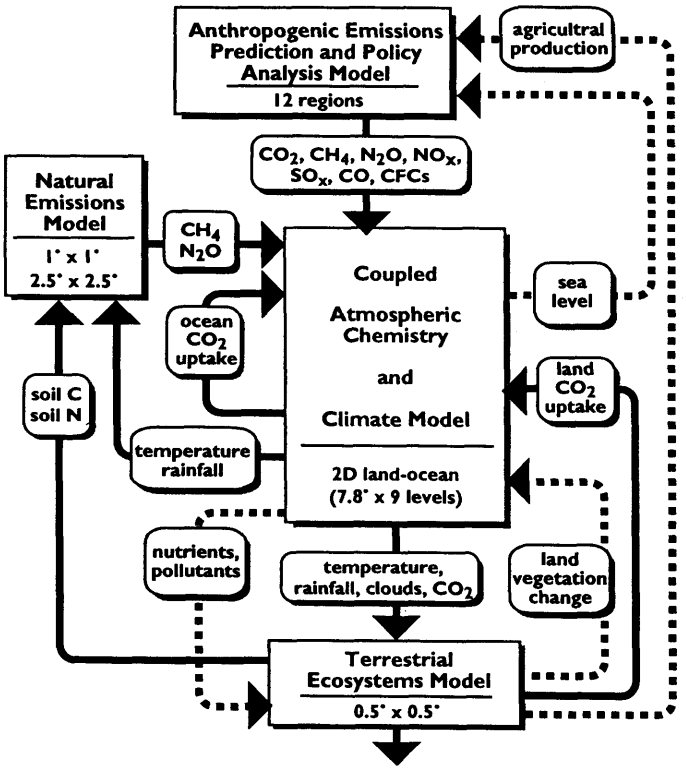

Fig. 1. The component models of the integrated assessment framework at Massachusetts Institute of Technology. Linkage and feedbacks between the component models which are currently included or under development for future inclusion are shown as solid lines and dashed lines, respectively.

climate model and the 3-D GCMs for an effective doubling of CO_2.

2. Description of the terrestrial ecosystem model (TEM)

The TEM (Raich et al., 1991; McGuire et al., 1992, 1993, 1995) is a process-based ecosystem model that simulates important carbon and nitrogen fluxes and pools for various terrestrial ecosystems (Fig. 2). It runs at a monthly time step. Driving variables include monthly climate (precipitation, mean temperature and mean cloudiness), soil texture (proportion of sand, clay and silt), elevation, vegetation and water availability. The water balance model of Vorosmarty et al. (1989) is used to generate hydrological inputs (e.g., PET, soil moisture) for TEM. For global extrapolation, TEM uses spatially explicit data sets that are gridded at a resolution of 0.5° latitude by 0.5° longitude (about 55 km × 55 km at the equator). The global data sets include long-term average climate data (Wolfgang Cramer, personal communication), potential vegetation (Melillo et al., 1993), soil texture (FAO/CSRC/MBL, 1974) and elevation (NCAR/Navy, 1984). These data sets contain 62,483 land grid cells, including 3,059 ice grid cells and 1,525 wetland grid cells. Geographically, the global data sets cover land areas between 56°S and 83°N.

In this study, we use TEM version 4.0, which was modified from TEM version 3 to improve patterns of soil carbon storage along gradients of temperature, moisture and soil texture (see McGuire et al., 1995; VEMAP Members 1995, Pan et al., 1996). Version 3 of TEM has been used to examine the response of NPP and carbon storage to changes in climate and atmospheric CO_2 concentration (McGuire et al., 1993; Melillo

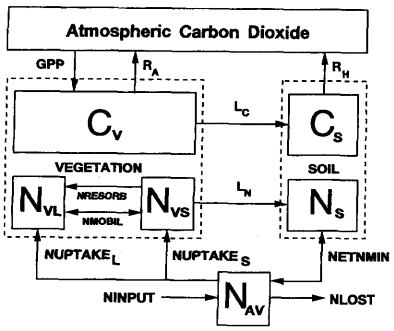

Fig. 2. The terrestrial ecosystem model (TEM). The state variables are: carbon in vegetation (C_V); structural nitrogen in vegetation (N_{VS}); labile nitrogen in vegetation (N_{VL}); organic carbon in soils and detritus (C_S); organic nitrogen in soils and detritus (N_S); and available soil inorganic nitrogen (N_{AV}). Arrows show carbon and nitrogen fluxes: GPP, gross primary productivity; R_A, autotrophic respiration; R_H, heterotrophic respiration; L_C, litterfall carbon; L_N, litterfall nitrogen; $NUPTAKE_S$, N uptake into the structural N pool of the vegetation; $NUPTAKE_L$, N uptake into the labile N pool of the vegetation; NRESORB, N resorption from dying tissue into the labile N pool of the vegetation; NMOBIL, N mobilized between the structural and labile N pools of the vegetation; NETNMIN, net N mineralization of soil organic N; NINPUT, N inputs from the outside of the ecosystem; and NLOST, N loss from the ecosystem. (From Melillo et al., 1993, reprinted with permission from *Nature* **363**, 234–240, © 1993 MacMillan Magazines Limited.)

et al., 1993, 1994, 1995). The primary difference between the two versions of TEM is how the pool of soil organic matter is defined. The version 4.0 of TEM defines a reactive soil carbon pool that excludes biologically unreactive soil organic matter. Thus, the pool only considers soil carbon that is potentially responsible to climate change. Globally, the reactive soil carbon pool estimated by version 4.0 is approximately 1/2 of the total soil carbon estimated by version 3 of TEM (see Melillo et al., 1995 and McGuire et al., 1995). Other modifications in TEM 4.0 include changes in the algorithms describing: (1) temperature effects on gross primary production, (2) moisture effects on nitrogen uptake by plants and microbes, (3) decomposition of soil organic matter, and (4) the factors influencing the carbon to nitrogen ratio of vegetation in grasslands. In TEM 4.0, soil texture is treated as a continuous variable based on the proportion of silt plus clay, rather than a categorical variable with 5 classes (i.e., sand, sand loam, loam, clay loam, and clay). More model parameters now depend on soil texture, including the carbon and nitrogen uptake capacity of vegetation and the decomposition and immobilization capacity of microbes. Plant rooting depth, porosity, field capacity and wilting point are also dependent upon a continuous soil texture variable.

In this study, we focus on NPP and total carbon storage, which are two important variables in impact assessment. Total carbon storage is the sum of vegetation carbon and reactive soil organic carbon. Net primary production (NPP) is calculated as the difference between gross primary production (GPP) and plant respiration (R_A). The flux R_A, which includes both maintenance respiration and construction respiration, is calculated at each monthly time step as a function of temperature and vegetation carbon. The flux GPP is calculated at each monthly time step as follows:

$$\mathrm{GPP} = C_{max} f(\mathrm{PAR}) f(\mathrm{LEAF}) f(\mathrm{T}) \times f(\mathrm{CO_2}, \mathrm{H_2O}) f(\mathrm{NA}),$$

where C_{max} is the maximum rate of C assimilation, PAR is photosynthetically active radiation, LEAF is leaf area relative to maximum annual leaf area, T is temperature, CO_2 is atmospheric CO_2 concentration, H_2O is water availability, and NA is nitrogen availability (Raich et al., 1991; McGuire et al., 1992).

3. Description of the 2-D atmospheric model

The atmospheric model used in this study is a modified version of the two-dimensional (zonally averaged) statistical-dynamical model developed by Yao and Stone (see Yao and Stone, 1987; Stone and Yao, 1987, 1990). The grid used in the model consists of 24 points in latitude, corresponding to a resolution of 7.826°; and nine layers in the vertical: two in the planetary boundary layer, five in the troposphere, and two in the stratosphere. The original version of the 2-D model was developed from the GISS GCM. Thus, the model's algorithms and parameterizations of physical processes, such as radiation, convection, and so on, are similar to those described in Hansen et al. (1983).

The main difference between the original model and the modified version of the 2-D model used

here is the treatment of the lower boundary. In the original model the entire earth's surface was defined as ocean, while in the modified version the real land/ocean distribution is taken into account. The modified version of the 2-D model, as well as the GISS GCM, allows up to four different kinds of surfaces to exist in the same grid cell: open ocean, ocean-ice, land and land-ice. The surface characteristics, such as temperature and soil moisture, as well as turbulent surface fluxes are calculated separately for each kind of surface. At the same time, the atmosphere is assumed to be well mixed zonally, that is, air temperature, humidity and so on are the same throughout a latitudinal band. As a result, the model gives the same values of precipitation and clouds for land and ocean at each latitude. A detailed description of the modified model is given in Sokolov and Stone (1995). The results of the present climate simulations performed with this version of the 2-D model have been compared with observational data and with the results of analogous simulations with the GISS GCM (Sokolov and Stone, 1995). The comparisons show that the MIT 2-D model reasonably reproduces the zonally averaged characteristics of the present climate.

For the simulation of climate change associated with a doubling of atmospheric CO_2 concentration, the atmospheric model has been coupled with a mixed layer ocean model. The latter includes the so called Q-flux (or heat flux) correction term which represents the horizontal oceanic heat transport and heat exchange between the mixed layer and the deep ocean, but can also compensate for deficiencies in the atmospheric model. The values of the Q-flux were calculated from the results of a present-day climate simulation with climatological sea surface temperature and sea-ice distribution (see Russell et al., 1985). The same values of the Q-flux term are used in the simulations with both present and doubled CO_2 concentration, which means that no ocean heat transport feedback is permitted. Sea-ice distribution (depth and cover) have been calculated by the simple thermodynamical model described in Hansen et al. (1984). The same approach for sea surface temperature and sea-ice calculation was also used in the doubled CO_2 climate change simulations with the GISS and GFDL-q GCMs.

Despite the use of a Q-flux in the mixed layer ocean model, there are some differences between prescribed values of sea surface temperature, sea ice cover and sea ice depth and those calculated in the present climate simulation with the coupled model. A detailed analysis of climate feedbacks has shown that the surface albedo feedback, associated mainly with changes of snow and sea ice cover, produced by the 2D model is twice as large as that for the GISS GCM (Sokolov and Stone, 1994). The strong sea ice feedback is caused, in part, by the above mentioned differences in the sea ice simulation. Consequently, surface temperature changes produced by this version of the 2-D model in high latitudes are larger than those in the simulations with the GISS and GFDL GCMs (Fig. 3a). However, the global average values and latitudinal distributions (except high latitudes) of climate variables of the 2-D model's responses to doubled atmospheric CO_2 concentration are within the range produced by the GCMs (see Fig. 3).

4. Climate change scenarios and atmospheric CO_2 concentration

We used climate outputs for $1 \times CO_2$ and $2 \times CO_2$ simulations from two 3-D GCMs, i.e., GISS (Hansen et al., 1983), GFDL-q (Wetherald and Manabe, 1988); and the 2-D MIT L-O climate model (Sokolov and Stone, 1995). The spatial resolution (longitude $\times$ latitude) is $10.0° \times 7.826°$ for GISS and $7.5° \times 4.44°$ for GFDL-q. Atmospheric models and terrestrial ecosystem models operate at very different temporal and spatial scales (Aber, 1992). The structure of the terrestrial biosphere is enormously heterogeneous in space, because of topography, elevation, soils and climate. Therefore, the climate outputs from GISS and GFDL-q were interpolated to $0.5° \times 0.5°$ grid cells by applying a spherical interpolation routine to the data (Willmott et al., 1985). We generated "future climate" by (1) adding the absolute difference in monthly temperature between $2 \times CO_2$ and $1 \times CO_2$ simulations to the contemporary monthly temperature data; (2) multiplying the ratio in monthly precipitation between $2 \times CO_2$ and $1 \times CO_2$ simulations to the contemporary monthly precipitation data; and (3) multiplying the ratio in monthly cloudiness between $2 \times CO_2$ and $1 \times CO_2$ simulations to the contemporary monthly cloudiness data. For the 2-D MIT L-O

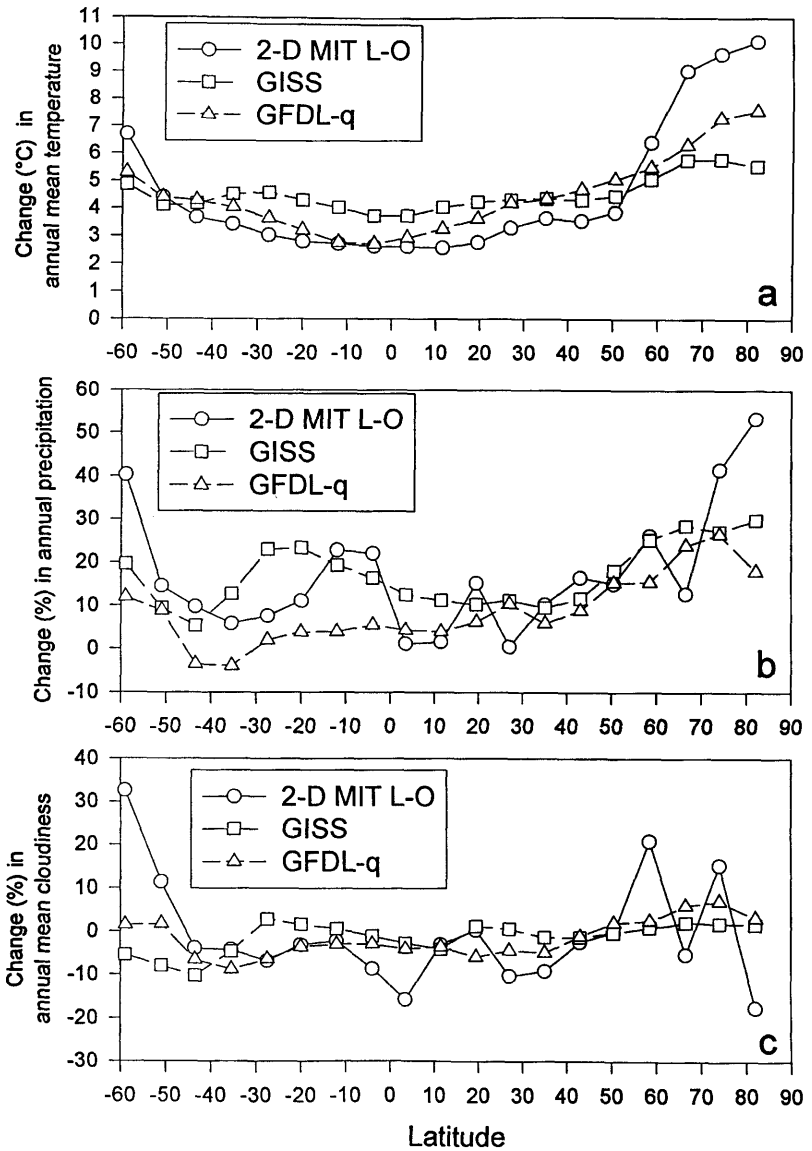

Fig. 3. The zonal mean changes over land of annual mean temperature, annual precipitation and annual mean cloudiness between $1 \times CO_2$ and $2 \times CO_2$ simulations by the 2-D MIT L-O climate model and the 3-D GISS and GFDL-q GCMs along the latitudinal bands as defined by the 2-D MIT L-O climate model. The GCMs outputs are averaged over the same latitudinal bands as those of the 2-D MIT L-O climate model.

climate model, the absolute differences in monthly temperature and the ratios of monthly precipitation and monthly cloudiness between the $2 \times CO_2$ and $1 \times CO_2$ simulations were calculated for each latitudinal band. We then applied the zonally averaged data over land to all the $0.5° \times 0.5°$ grid cells within the latitudinal band. By generating "future climate" in this way, we have assumed that general patterns of climate within a latitudinal band will remain unchanged. For the contemporary climate, we used the long-term monthly average data of precipitation, temperature and

cloudiness from the Cramer and Leemans CLIMATE database (Cramer, personal communication). The Cramer and Leemans climate database is an update of the Leemans and Cramer (1991) climate database, and has been developed using more weather stations and a new algorithm for spatial interpolation.

The GISS GCM and MIT L-O climate model simulated climate conditions for "current" CO_2 ($1 \times CO_2$, 315 ppmv) and doubled "current" CO_2 ($2 \times CO_2$, 630 ppmv), respectively. The GFDL-q GCM used 300 ppmv CO_2 as the $1 \times CO_2$ and 600 ppmv CO2 as the $2 \times CO_2$. Projected changes in global mean annual temperature vary little among the three climate models: +4.0°C for GFDL-q, +4.2°C for GISS and +4.2°C for MIT L-O. Global annual precipitation increases by +8.3% for GFDL-q, +11.0% for GISS and +11.5% for MIT L-O. Projected decrease of global annual mean cloudiness is largest (−3.4%) for GISS, intermediate (−2.6%) for MIT L-O and lowest (−0.7%) for GFDL-q. All three models predict small increases of annual mean temperature at low latitudes and larger increase at high latitudes (Fig. 3a). There are large latitudinal variations in annual precipitation and annual mean cloudiness for each of the climate models (Fig. 3b, 3c).

Atmospheric CO_2 concentration has increased since the pre-industrial period from about 280 ppmv in 1800 to 356 ppmv in 1993. The additional radiative forcing due to this CO_2 increase is 1.56 W/m^2, accounting for approximately 63% of the total additional radiative forcing by the long-lived greenhouse gases (CO_2, CH_4, N_2O and halocarbons) (IPCC, 1994, 1995). Atmospheric concentrations of other greenhouse gases (e.g., CH_4, N_2O, halocarbons) are also increasing. According to the emission scenarios projected by the economic-emission model in the MIT integrated assessment framework, the radiative forcing from CO_2 accounts for about 76% of the total additional radiative forcing equivalent to a doubling of atmospheric CO_2 concentration (from 315 ppmv to 630 ppmv). Similarly, other studies have also projected that CO_2 is still the dominant long-lived greenhouse gas in the next century and that its added radiative forcing contributes between 76% and 84% of the total additional radiative forcing (IPCC, 1995). An "effective CO_2 doubling" has been defined as the combined radiative forcing of all greenhouse gases having the same forcing as doubled CO_2 (Rosenzweig & Parry, 1994). Therefore, we used 522 ppmv CO_2 in the simulations with TEM as the physiologically relevant CO_2 level that corresponds to an effective CO_2 doubling.

Unlike CH_4 and N_2O, CO_2 has a direct effect on carbon uptake and accumulation in terrestrial ecosystems. A number of experimental studies have shown that photosynthesis and water use efficiency of plants are enhanced under elevated CO_2 levels (Kimball, 1975; Idso and Kimball, 1993; Owensby et al., 1993; Polley et al., 1993; Idso and Idso, 1994). Previous simulations with TEM indicate that doubling atmospheric CO_2 concentration alone can potentially increase global NPP and carbon storage (Melillo et al., 1993, 1995; McGuire et al., 1995). The interaction between CO_2 and climate change also affects the responses of NPP and carbon storage, as modeled in TEM (Melillo et al., 1993, 1995; McGuire et al., 1993, 1995). Therefore, it is more appropriate to use an effective doubling of CO_2, when examining the responses of terrestrial ecosystems to changes in climate and atmospheric CO_2 concentration.

To determine responses of the terrestrial biosphere to climate change with elevated CO_2, we ran TEM for (1) contemporary climate with 315 ppmv CO_2; and (2) climate change with 522 ppmv CO_2. The TEM simulation driven by contemporary climate with 315 ppmv CO_2 (corresponding to atmospheric CO_2 concentration in 1957) is the baseline or reference. We ran TEM to its equilibrium state, i.e., all annual carbon and nitrogen fluxes of an ecosystem are balanced within each grid cell. Therefore, the estimates of carbon and nitrogen fluxes and pool sizes apply only to mature, undisturbed vegetation and ecosystems. In this study, we have not considered the effects of land use and management on carbon and nitrogen dynamics.

5. Results

5.1. *NPP and total carbon storage under contemporary climate and 315 ppmv CO_2*

For contemporary climate with 315 ppmv CO_2, TEM estimates global terrestrial annual net primary production (NPP) to be 47.9 PgC/yr. Cumulative NPP in tropical regions is estimated

to be as much as two times higher than cumulative NPP in temperate regions (Fig. 4a). Tropical evergreen forests account for 34% of global NPP, although its area is about 14% of the global land area used in the simulations (Table 1). Tropical ecosystems (tropical evergreen forest, tropical deciduous forest, xeromorphic forest and tropical savanna) account for 57% of global NPP. Cumulative NPP is low in high latitude ecosystems in the northern hemisphere (Fig. 4a), where NPP is primarily limited by low temperature and consequently low nitrogen availability. Polar desert/alpine tundra and moist tundra ecosystems occur over 8% of the global land area but account for only 2% (0.8 PgC/yr) of global NPP (Table 1). Together, boreal forests and boreal woodlands account for 14.5% of the global land area and their annual NPP is about 8% (3.8 PgC/yr) of global NPP. In arid regions (arid shrubland and desert), NPP is limited by water

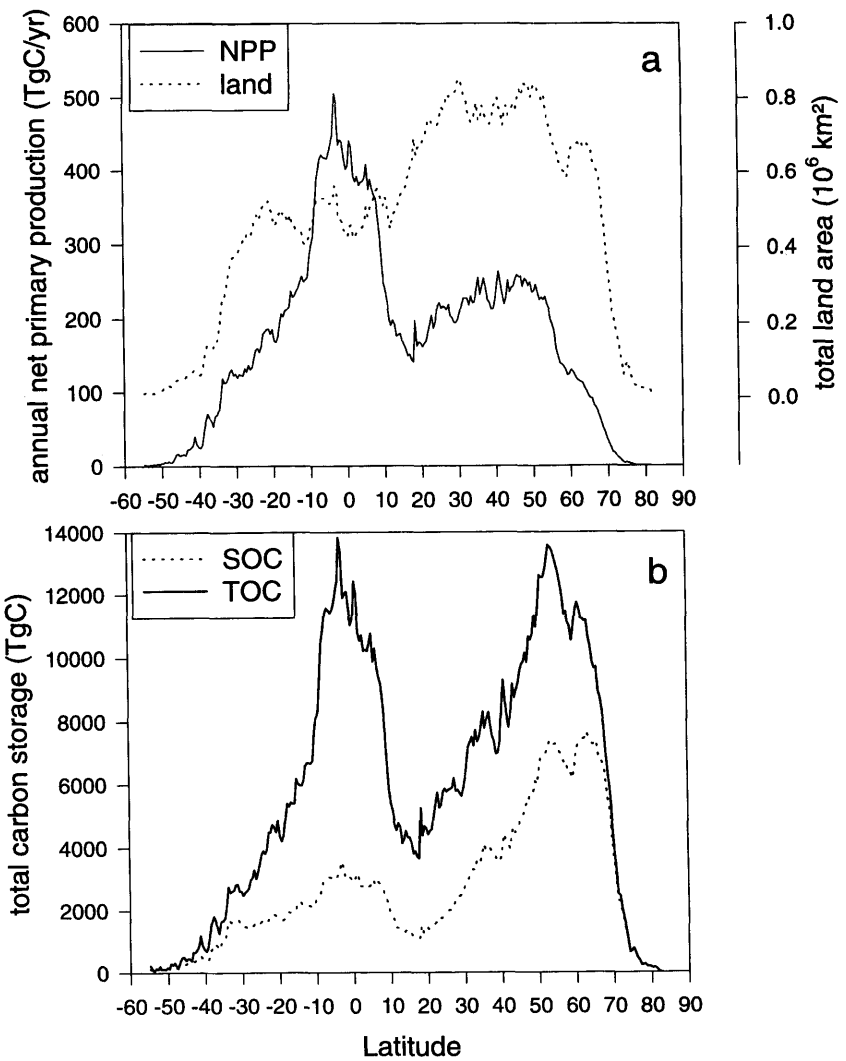

Fig. 4. Latitudinal distributions (0.5° resolution) of (a) annual net primary production (NPP), (b) reactive soil organic carbon (SOC) and total carbon storage (TOC) for contemporary climate with 315 ppmv atmospheric CO_2 concentration. Carbon storage in vegetation is the difference between total carbon storage and reactive soil organic carbon.

Table 1. *Estimates of annual net primary production and total carbon storage for contemporary climate (contemp) at 315 ppmv CO_2 and their equilibrium responses to changes in climate at 522 ppmv CO_2*

			Annual net primary production				Total carbon storage			
Vegetation type	Number of cell	Area (10^6 km^2)	Contemp (Pg C/yr)	MIT L-O (%)	GISS (%)	GFDL-q (%)	Contemp (Pg C)	MIT L-O (%)	GISS (%)	GFDL-q (%)
polar desert/alpine tundra	3,758	5.3	0.3	25.5	30.7	29.7	36	−2.5	2.3	1.6
wet/moist tundra	4,207	5.2	0.5	25.3	31.7	30.5	63	−5.7	0.8	−0.3
boreal woodland	4,545	6.5	1.0	20.6	29.7	29.3	101	4.8	11.0	11.2
boreal forest	7,577	12.5	2.8	20.1	25.0	26.8	251	−3.9	7.8	7.1
temperate coniferous forest	1,126	2.5	1.0	22.6	21.0	22.0	43	9.7	11.1	8.8
desert	4,170	11.6	0.4	36.5	41.5	28.0	7	7.7	4.8	4.8
arid shrubland	5,784	14.7	1.5	30.1	33.5	25.3	33	12.3	13.3	12.4
short grassland	2,067	4.7	1.0	24.1	29.0	27.7	20	0.5	1.5	−0.7
tall grassland	1,567	3.6	1.2	21.5	28.0	24.0	18	1.6	1.3	−0.3
temperate savanna	2,921	6.8	2.4	21.5	25.0	23.7	74	9.4	8.7	9.0
temperate deciduous forest	1,666	3.7	2.4	21.1	23.0	22.6	92	8.4	6.5	0.8
temperate mixed forest	2,320	5.2	3.0	20.5	21.6	20.1	114	6.8	8.3	5.9
temperate broadleaf evergreen forest	1,268	3.3	2.8	17.4	16.7	20.3	74	7.1	7.4	8.0
mediterranean shrubland	575	1.5	0.4	22.9	27.3	22.0	11	11.9	9.3	10.1
tropical savanna	4,666	13.9	5.7	14.7	21.1	15.0	124	5.8	7.0	2.4
xeromorphic forest	2,387	6.9	2.4	21.4	23.7	19.5	49	11.7	12.2	10.2
tropical deciduous forest	1,607	4.7	2.8	12.7	15.0	13.7	82	10.5	7.8	11.9
tropical evergreen forest	5,868	17.8	16.3	14.2	15.5	13.6	467	16.0	15.2	4.2
total	57,899	130.3	47.9	17.8	20.6	18.5	1,658	6.9	8.7	8.3

availability. Cumulative NPP in arid regions accounts for 4% of global NPP, although the area of arid regions is about 20% of the global land area.

The TEM estimates total terrestrial carbon storage (vegetation carbon plus reactive soil organic carbon) of the globe to be 1658 PgC: 908 PgC in vegetation carbon and 750 PgC in soils; the estimate of vegetation carbon does not consider the conversion of forests to agriculture and the estimate of soil organic carbon excludes inert soil organic matter. Total carbon storage has a bimodal distribution across latitude with highest storage in the tropical and boreal regions (Fig. 4b). About 43% of global total carbon storage occurs in tropical ecosystems, where most of the carbon is stored in vegetation. Of the 18 biomes, tropical evergreen forest accounts for the largest portion (about 28%) of global total carbon storage (Table 1). Total carbon storage of polar desert/alpine tundra and moist/wet tundra is 99 PgC, about 6% of global total carbon storage. Boreal forest and boreal woodlands account for about 21% (352 PgC) of global total carbon storage. A large proportion of the carbon in the northern high latitudes is stored as soil organic carbon (Fig. 4b). Because of low temperature in temperate and high latitudes, soil organic matter decomposes slowly and has accumulated over centuries.

5.2. *Response of NPP to climate change and elevated CO_2*

The TEM estimates that global NPP increases substantially for climate change with 522 ppmv CO_2 but varies little among the three climate change predictions: +17.8% (8.6 PgC/yr) for the MIT L-O climate, +18.5% (8.9 PgC) for the GFDL-q climate and +20.6% (9.9 PgC) for the GISS climate (Table 1). At the 0.5° resolution, the latitudinal response of cumulative NPP has a bimodal distribution with the largest increases in both tropical forest regions and the temperate ecosystems of the Northern hemisphere (Fig. 5a). Generally, the latitudinal distribution of changes in NPP under the MIT L-O climate is similar to those under the GISS and GFDL-q climate, except for relatively large differences within the 50.5°N–58.5°N and 66.5°N–74.0°N bands (Fig. 5a). In the 50.5°N–58.5°N band, the difference in NPP response is caused by the difference in the projected change in annual mean cloudiness which is over 20% higher in the MIT L-O predictions than in the GISS and GFDL-q predictions (Fig. 3c). Higher cloudiness reduces photosynthetically active radiation, which causes reduced gross primary production. In the 66.5°N–74°N band, projected changes in mean annual cloudiness and mean annual temperature by the MIT L-O model are over 10% and 2°C higher than those by the GISS and GFDL-q models (Fig. 3a,c). Higher temperature tends to increase decomposition of soil organic matter in these regions, which releases more N from soils for plant uptake, and thus NPP may increase (see Melillo et al., 1993). Higher temperature also increases evapotranspiration, which reduces soil moisture, and thus NPP may decrease because of water stress to vegetation. The lower NPP responses in these high latitude regions appear to be caused by both stronger water stress and lower photosynthetically active radiation.

Cumulative NPP for each of the 18 biomes increases between 13% and 42% (Table 1). The percent NPP increase is higher in arid ecosystems than in temperate and tropical forest ecosystems (Table 1). The NPP of arid ecosystems is primarily limited by water. In TEM, a direct effect of elevated CO_2 is to increase the intercellular CO_2 concentration within a canopy, which potentially increases GPP via a Michaelis-Menton (hyperbolic) relationship. Elevated CO_2 significantly increases water use efficiency of arid ecosystems. Tropical ecosystems are not limited by nitrogen availability because of high rate of net nitrogen mineralization. Elevated CO_2 results in considerable increase of NPP in tropical ecosystems. In contrast, NPP of moist temperate and high latitude ecosystems is primarily limited by nitrogen availability. Climate change affects NPP in a number of ways. Higher temperature enhances plant respiration and potential evapotranspiration (PET). Higher PET reduces soil moisture and thus causes water stress to plants, so that NPP decreases. Increased temperature and precipitation may also enhance decomposition of soil organic matter to release more nitrogen from the soils for plant uptake, so that NPP increases (McGuire et al., 1992, 1993). It is the balance among the effects of CO_2, climate and nitrogen that determines the various response of NPP in different ecosystems.

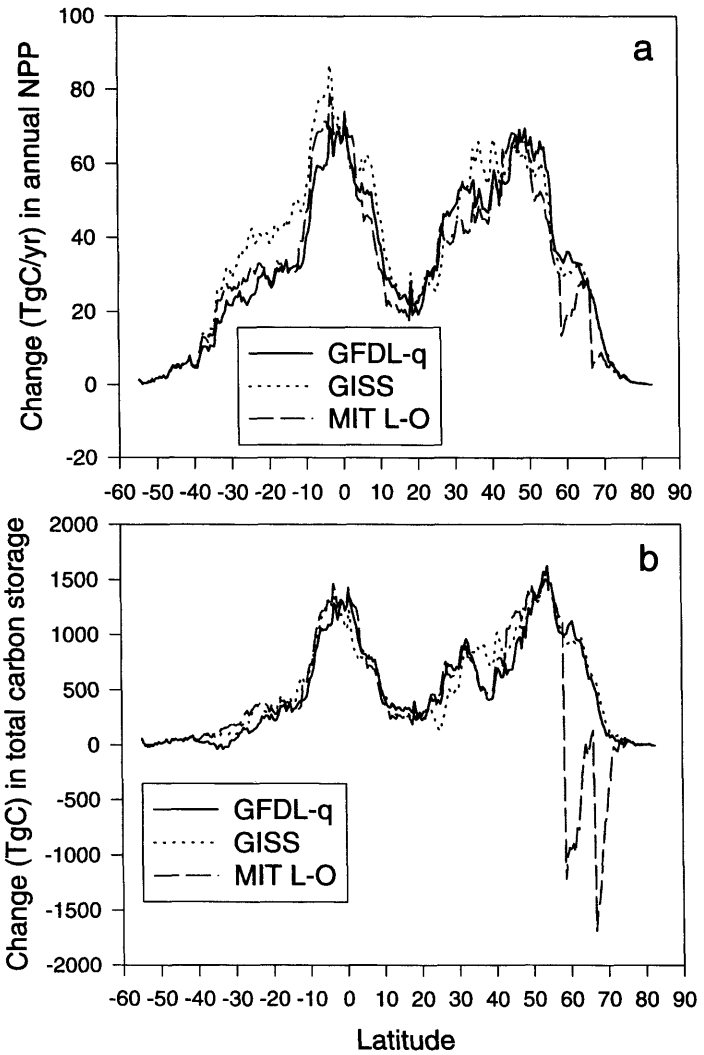

Fig. 5. Latitudinal distributions (0.5° resolution) of the projected changes in (a) annual net primary production (NPP) and (b) total carbon storage for the 2-D MIT L-O climate and the 3-D GISS and GFDL-q climates with 522 ppmv CO_2.

Cumulative NPP for most of the 18 biomes varies only slightly among the three climate change predictions (Table 1). The NPP responses in the high latitude regions (boreal forest, boreal woodland, wet/moist tundra, polar desert/alpine tundra) are exceptions, where the responses under the MIT L-O climate are 4% to 9% lower than those under the GISS and GFDL-q climates. This is mostly attributable to the relatively larger increases of temperature and cloudiness in the high-latitude regions, as projected by the MIT L-O model (Fig. 3a,c).

The mean biome NPP increases considerably for each of the 18 biomes, but varies little (within $\pm 1\%$) among the three climate change predictions for most of the biomes (Table 2). The differences in mean biome NPP between the 2-D MIT L-O climate and the 3-D GISS and GFDL-q climates reflect the differences in cumulative NPP, as the mean biome NPP estimated under the 2-D MIT

Table 2. *Area-weighted mean and standard deviation (stddev) of annual net primary production for contemporary climate at 315 ppmv CO_2 and different climate change scenarios at 522 ppmv CO_2*

	Contemporary climate		MIT L-O		GISS		GFDL-q	
Vegetation type	mean ($gC/m^2/yr$)	stddev	mean ($gC/m^2/yr$)	stddev	mean ($gC/m^2/yr$)	stddev	mean ($gC/m^2/yr$)	stddev
polar desert/alpine tundra	62	24	77	27	81	29	80	28
wet/moist tundra	103	29	129	32	135	31	134	33
boreal woodland	157	31	189	38	204	37	203	34
boreal forest	228	36	274	48	285	41	289	43
temperate coniferous forest	397	126	487	138	481	129	484	142
desert	34	28	47	36	49	38	44	34
arid shrubland	99	41	128	53	132	52	124	50
short grassland	221	71	274	84	284	89	281	80
tall grassland	330	166	401	192	423	207	409	186
temperate savanna	348	131	423	156	435	154	430	154
temperate deciduous forest	661	108	800	116	812	126	810	130
temperate mixed forest	570	117	686	127	693	133	684	135
temperate broadleaf evergreen forest	828	235	973	243	966	244	996	248
mediterranean shrubland	304	130	373	158	386	155	370	151
tropical savanna	411	183	472	206	498	217	473	207
xeromorphic forest	354	182	430	209	438	208	423	208
tropical deciduous forest	588	209	663	238	676	236	669	230
tropical evergreen forest	916	183	1,046	224	1,059	217	1,041	219
globe	368	292	434	334	444	336	436	333

L-O climate are within 4–6% for tundra and boreal forest, and 7–8% for boreal woodland less than the corresponding estimates under the GISS and GFDL-q climates. Also, the standard deviations of annual NPP for each of the 18 biomes vary little among the three climate change predictions (Table 2). This indicates that the variability of NPP responses for grid cells within a biome is similar among the three climate change predictions.

5.3. *Response of total carbon storage to climate change and elevated CO_2*

For climate change with 522 ppmv CO_2, TEM estimates that total carbon storage of the globe increases moderately: +6.9% (115 PgC) for the MIT L-O climate, +8.3% (137 PgC) for the GFDL-q climate and +8.7% (144 PgC) for the GISS climate. The responses of vegetation carbon and soil organic carbon differ significantly from each other. Global vegetation carbon increases substantially: +17.3% (157 PgC) for the MIT L-O climate, +18.3% (166 PgC) for the GFDL-q climate and +19.5% (177 PgC) for the GISS climate. In contrast, the pool of reactive soil organic carbon decreases moderately, i.e., −5.6% (42 PgC) for the MIT L-O climate, −4.4% (33 PgC) for the GISS climate and −3.9% (29 PgC) for the GFDL-q climate.

At the 0.5° resolution, the latitudinal response of total carbon storage to climate change has a bimodal distribution with the largest increase in the northern temperate regions and tropical regions (Fig. 5b). The response of total carbon storage under the MIT L-O climate is similar to the responses of total carbon storage under the GISS and GFDL-q climates, except for the large differences within the 50.5°N–58.5°N and 66.5°N–74.0°N bands (Fig. 5b). Within these two latitudinal bands, the MIT L-O model projects relatively higher temperature and cloudiness than the GISS and GFDL-q models. Higher temperature increases the loss of soil organic carbon, while higher cloudiness causes a decrease in the response of vegetation carbon because of lower annual NPP.

The response of total carbon storage varies substantially among the 18 biomes (Table 1). For the MIT L-O climate, the response of total carbon storage ranges from a decrease of 5.7% in wet/moist tundra to an increase of 16.0% in desert. For the GISS climate, total carbon storage increases from 0.8% in wet/moist tundra to 15.2% in desert. For the GFDL-q climate, total carbon storage ranges from a decrease of 0.7% in tall grassland to an increase of 12.4% in temperate deciduous forest (Table 1). Responses of total carbon storage for most of the 18 biomes are similar among the three climate change predictions (Table 1). The largest difference in the response of total carbon storage among the climate change predicitons occurs in boreal forest. The TEM estimates that total carbon storage of boreal forest has a decrease of 9.8 PgC (3.9%) for the MIT L-O climate but an increase of 17.8 PgC (7.1%) for the GFDL-q climate and 19.6 PgC (7.8%) for the GISS climate. As described earlier, the different responses of total carbon storage of boreal forest are attributable to the higher temperature and cloudiness increases projected by the 2-D MIT L-O climate model at high latitudes.

The mean total carbon storage varies little (within ±2%) among the three climate change predictions for most of the biomes (Table 3). Again, the differences in the mean total carbon storage between the 2-D MIT L-O climate and the 3-D GCMs climates are large for the biomes in the northern high latitude: within ±(5–7)% for tundra and boreal forest and ±(11–12)% for boreal woodland. Also, the standard deviations of total carbon storage for each of the 18 biomes vary little among the three climate change predictions (Table 3). This again indicates that the variability of the grid cell response of total carbon storage within a biomes is similar among the three climate change predictions.

6. Discussion

6.1. *Contemporary climate, NPP and total carbon storage*

A number of studies have estimated global NPP under contemporary climate, by either extrapolating field data or using modeling approaches. For the 13 estimates of global NPP summarized by Melillo (1994), global NPP has a mean of 57 PgC/yr and a standard deviation of 17.4 PgC/yr. Our estimate of global NPP (47.9 PgC/yr) under contemporary climate with 315 ppmv CO_2 is very close to the estimate (48.2 PgC/yr) by Whittaker and Likens (1973). Potter et al. (1993) estimated 48 PgC/yr of global

Table 3. *Area-weighted mean and standard deviation (stddev) of total carbon storage for contemporary climate at 315 ppmv CO_2 and different climate change scenarios at 522 ppmv CO_2*

	Contemporary climate		MIT L-O		GISS		GFDL-q	
Vegetation type	mean (gC/m^2)	stddev	mean (gC/m^2)	stddev	mean (gC/m^2)	stddev	mean (gC/m^2)	stddev
polar desert/alpine tundra	6,890	2,042	6,711	1,987	7,041	2,087	6,995	2,093
wet/moist tundra	12,112	2,299	11,388	2,231	12,178	2,109	12,043	2,095
boreal woodland	15,597	2,296	14,995	2,874	16,816	2,485	16,710	2,306
boreal forest	20,096	2,487	21,050	3,683	22,299	2,501	22,341	2,799
temperate coniferous forest	17,412	3,905	19,466	4,143	19,008	3,984	19,159	4,349
desert	577	647	669	687	664	693	601	637
arid shrubland	2,272	1,431	2,463	1,504	2,421	1,476	2,291	1,426
short grassland	4,339	1,170	4,397	1,160	4,381	1,169	4,313	1,185
tall grassland	4,962	1,542	4,985	1,506	5,036	1,503	4,929	1,457
temperate savanna	10,792	4,331	11,834	4,612	11,991	4,595	11,738	4,730
temperate deciduous forest	25,122	3,417	28,223	3,641	28,463	3,755	28,243	4,033
temperate mixed forest	21,636	3,211	24,174	3,539	24,266	3,519	23,851	3,781
temperate broadleaf evergreen forest	22,302	5,195	24,634	5,142	24,049	5,007	24,967	5,203
mediterranean shrubland	7,401	3,365	7,833	3,530	7,916	3,406	7,577	3,393
tropical savanna	8,942	3,672	9,554	3,877	9,685	3,867	9,467	3,857
xeromorphic forest	7,129	4,022	7,680	4,121	7,468	3,957	7,468	4,068
tropical deciduous forest	17,402	6,441	18,644	6,970	18,683	6,696	18,790	6,736
tropical evergreen forest	26,267	5,121	28,745	6,007	28,559	5,713	28,625	6,904
globe	12,728	8,779	13,609	9,651	13,835	9,681	13,777	9,773

NPP, using remote sensing data from 1987 and climate data.

The global NPP estimate (47.9 PgC/yr) in this study is slightly lower than the estimate (51.0 PgC/yr) in an earlier study (Melillo et al., 1993), which used version 3 of TEM, precipitation and temperature data from Legates and Willmott (1988), and cloudiness data from Hahn et al. (1988). In general, the Cramer and Leemans climate data used in this study represent a cooler, drier and sunnier world than the data from Legates and Willmott (1988) and Hahn et al. (1988). For the Cramer and Leemans climate dataset, global average annual mean temperature, annual precipitation and cloudiness over land are 12.8°C, 795 mm and 46%, respectively. The Legates and Willmott dataset has a global mean annual temperature of 13.8°C and global average annual precipitation of 845 mm, while the Hahn dataset has a global average annual cloudiness of 56%. The differences in temperature and precipitation between the Cramer and Leemans dataset and the Legates and Willmott dataset are relatively small in tropical regions but large in temperate and high latitudes.

The estimate of total carbon storage (1658 PgC) of the terrestrial biosphere in this study is also lower than the estimate (2279 PgC) in an earlier study using TEM version 3 (Melillo et al., 1995), in which the estimate of soil carbon pool includes inert soil organic matter. In previous studies TEM estimates that the unreactive soil organic matter pool is between 400 and 500 PgC (Melillo et al., 1995) and that land use reduces vegetation carbon stock between 150 and 200 PgC (D.W. Kicklighter, unpublished). Global reactive soil organic carbon estimated by TEM (750 PgC) in this study is about 50% of the approximately 1500 PgC estimated by several inventories of soil organic carbon to 1-meter depth (Schlesinger, 1977; Post et al., 1982; Eswaran et al., 1993). Because of the latitudinal distributions of vegetation carbon and reactive soil organic carbon, and the latitudinal gradients of temperature change, the response of total carbon storage to climate change may be dominated by vegetation in tropical regions but by soils in temperate and high latitude areas.

6.2. *Future climate, NPP and total carbon storage*

In an earlier study, TEM estimated global NPP responses to climate change with a doubling of CO_2 to be +25.1% for the GFDL-q climate and 25.9% for the GISS climate (Melillo et al., 1993), which are slightly higher than the responses of global NPP to climate change with 522 ppmv CO_2 in this study. The difference is mainly due to the larger increase of CO_2 concentration (from 312.5 ppmv to 625 ppmv) used in the earlier study (Melillo et al., 1993). The responses of NPP and total carbon storage to climate change with 522 ppmv CO_2 have bimodal distributions along the 0.5° resolution latitudinal gradient. This suggests that tropical regions and northern temperate regions may be two net sinks of terrestrial carbon storage with respect to ecosystem metabolism. The tropical sink of carbon storage may partially offset the carbon loss caused by land use change in tropical regions, e.g., deforestation.

The TEM results show that the responses of NPP and total carbon storage for the 2-D MIT L-O model and the 3-D GCM (GISS and GFDL-q) climate change calculations are similar to each other at the global, latitude and biome scales, except in high latitudes. The NPP responses for the 2-D MIT L-O climate are slightly closer to those for the GFDL-q climate than to those for the GISS climate, although the 2-D MIT L-O climate model was developed from the 3-D GISS climate model. The differences in estimates of NPP responses between the 2-D MIT L-O and the 3-D GCM climate change predictions are much smaller than the responses of NPP to climate change and elevated atmospheric CO_2 concentration.

There are relatively large differences in estimates of responses of NPP and total carbon storage between the 2-D MIT L-O climate and the 3-D GISS and GFDL-q climate at high latitudes in the northern hemisphere, where vegetation is dominated by tundra and boreal forest and woodland. These large differences highlight that NPP and total carbon storage in high latitudes are very sensitive to the changes in climate, particularly to the changes in temperature. Other studies have suggested that global warming is very likely to result in shrinkage of tundra and northward expansion of boreal and temperate ecosystems (Emanuel et al., 1985; Woodward and McKee, 1991; Cramer and Leemans, 1993). If forests move into the areas once occupied by tundra, carbon storage may increase in these areas because boreal and temperate forests store more carbon than tundra.

However, there is still large uncertainty about the magnitude of climate change at high latitudes. The effect of aerosols on radiative forcing of the atmosphere was not considered in the simulations of the 3-D GCMs and the 2-D L-O climate model. The predictions of climate changes at high latitudes are sensitive to the representation of the ocean and sea ice, and there is considerable uncertainty as to what is the correct way to parameterize sea-ice in climate models (Rind et al., 1995). Work is continuing to improve the 2-D MIT L-O climate model. Preliminary results have indicated that the 2-D climate model will estimate smaller changes in temperature at high latitudes, if the radiative fluxes and their impacts on surface temperature are calculated separately for the land (including snow) and ocean (including sea ice) fractions of a latitudinal band. The resultant changes in annual mean temperature at the high latitudes of the northern hemisphere for doubled CO_2 are about 2–3°C lower than the results of the 2-D climate model presented in this study (Fig. 3a). Thus, the discrepancy in temperature changes at the high latitudes between the 2-D climate model and the 3-D GCMs, as shown in Fig. 3, may be significantly reduced in future versions of the 2-D climate model. The 2-D climate model is also being coupled to an atmospheric chemistry model (Fig. 1). The combined chemistry/climate model is able to dynamically simulate the effect of aerosols on radiative forcing of the atmosphere (Ronald G. Prinn, personal communication).

6.3. *Policy making, NPP and carbon storage*

The Emissions Prediction and Policy Analysis model (EPPA in Fig. 1) in the MIT integrated framework, which is a significantly modified and improved version of the General Equilibrium Environmental (GREEN) model developed originally by the Organization for Economic Cooperation and Development (see OECD, 1992), divides the world into 12 economic regions. The EPPA model projects economic development and associated anthropogenic emissions of greenhouse gases in the 12 economic regions. Agriculture is one of the eight production sectors in the EPPA model. Further effort is needed to desegregate the agricultural sector, so that EPPA could handle a variety of crops and management options.

Aggregations of NPP and carbon storage responses to climate change over the 12 economic regions can provide an important linkage between ecosystems and the economy, which may have important implications to policy and decision making. We used potential vegetation in this study, which is our first step in coupling the TEM and the 2-D climate model. To examine the responses of NPP and carbon storage for potential vegetation and ecosystems provides a basis for us to investigate the impact of changes in land use and land cover on terrestrial ecosystems, including agro-ecosystems. At present, TEM has no estimates for net primary production and yields of cultivated lands. Development of a simplified crop model, which has a similar structure to TEM's and simulates carbon and nitrogen dynamics of a few major crops, is critically needed in the integrated assessment framework. Agricultural production in Fig. 1 includes livestock, forestry and crop productions. Properties of natural ecosystems have been taken into consideration in use and management of renewable natural resources. Stocking rate of livestock in rangelands is determined by NPP of rangelands. The dynamics of NPP and vegetation carbon are important in forestry production and management. Soil fertility, which is related to soil organic matter content and net nitrogen mineralization rate, influences yields and requirements for fertilizer applications of cultivated lands. In addition, biomass may play an increasing and significant role in global energy use in the next century (IPCC Working Group II, 1996).

Annual NPP for each of the 12 economic regions increases between 11% and 29%, and varies little among the three climate change predictions except for the former Soviet Union (Table 4). India, the Dynamic Asian Countries (e.g., South Korea, Thailand, Singapore) and Energy Exporting Countries (e.g., Egypt, Congo, Mexico, Iran, Iraq) have relatively smaller increase of annual NPP than the other economic regions. For most economic regions, the responses of annual NPP are slightly smaller under the MIT L-O climate than under the GISS and GFDL-q climate.

Similarly, the responses of total carbon storage are also close to each other among the three climate change predictions for all the economic regions except the former Soviet Union which has large areas of boreal forest and boreal woodland (Table 4). Total carbon storage in the former

Table 4. *Estimates of annual net primary production and total carbon storage in different economic regions for contemporary climate (contemp) at 315 ppmv CO_2 and their equilibrium responses to changes in climate at 522 ppmv CO_2*

			Annual net primary production				Total carbon storage			
Vegetation type	Number of cell	Area (10^6 km^2)	Contemp (Pg C/yr)	MIT L-O (%)	GISS (%)	GFDL-q (%)	Contemp (Pg C)	MIT L-O (%)	GISS (%)	GFDL-q (%)
USA	4,322	9.1	3.2	22.6	23.3	20.0	118	9.1	9.2	5.6
Japan	163	0.4	0.3	21.7	20.4	28.6	9	12.5	12.2	17.4
India	1,089	3.1	1.2	11.6	15.3	17.6	35	6.0	8.0	10.4
China	3,807	9.4	3.6	17.9	18.6	23.1	131	8.8	7.7	11.6
Brazil	2,726	8.2	6.3	15.9	16.9	14.8	6	15.9	16.9	14.8
EEC (European Community Countries)	1,109	2.4	1.3	23.6	23.5	22.6	45	13.5	13.2	11.2
EET (Eastern European Countries)	552	1.1	0.6	24.6	24.4	20.8	22	13.8	13.1	9.7
DAE (Dynamic Asia Economic)	330	1.0	0.8	11.2	11.4	12.5	22	6.7	5.9	8.1
OOE (Other OECD Countries)	10,841	20.0	4.7	23.2	25.1	22.7	231	7.1	8.6	8.0
FSU (Former Soviet Union)	13,467	21.1	4.2	20.8	28.0	28.1	296	-0.6	9.0	8.0
EEX (Energy Exporting Countries)	7,847	22.5	9.4	15.9	19.2	15.7	255	9.1	9.4	8.7
ROW (The Rest of the World)	11,646	32.1	12.4	16.0	19.8	15.7	330	7.6	7.9	6.6

Soviet Union decreases slightly (−0.6%) under the 2-D MIT L-O climate, but increases 8.0% under the GFDL-q climate and 9.0% under the GISS climate. As described earlier, this difference is caused by the larger increase of temperature and cloudiness at high latitudes of the MIT L-O climate.

7. Conclusions

Our analysis indicates that the 2-D MIT L-O climate model linked to a terrestrial ecosystem model such as TEM can provide very useful information on the responses of terrestrial primary production and carbon storage at large spatial scales, i.e., at scales of the globe, economic regions, and biomes. The differences in the responses of global NPP and total carbon storage between the linkage of TEM and the 2-D L-O climate model and the linkage of TEM and the 3-D GCMs are small and do not qualitatively affect the estimates of the impacts of climate change on biogeochemical cycles of the terrestrial biosphere at the global scale. At this stage of the 2-D climate model development, caution should be taken in assessing the impacts of climate change on NPP and total carbon storage at high latitudes of the northern hemisphere, because of the relatively large discrepancy in temperature changes for doubled CO_2 at high latitudes between the 2-D MIT L-O climate model and the 3-D GCMs.

Relative to 3-D GCMs, the 2-D L-O climate model is very computationally efficient, which means that the 2-D L-O climate model will allow many scenarios to be analyzed within the integrated assessment context. We can explore both economic and environmental consequences efficiently with the 2-D L-O climate model in the integrated assessment framework. The linkage between the 2-D L-O climate model and TEM will also enable us to efficiently explore the potential for the terrestrial biosphere to stabilize or destabilize the concentration of atmospheric CO_2 in transient experiments.

8. Acknowledgments

This study was supported by the MIT Joint Program on the Science and Policy of Global Change (CE-S-462041), DOE NIGEC (No:901214-HAR) and NASA EOS (NAGW-2669). We thank Ronald Prinn, Henry Jacoby, Richard Eckaus, Yude Pan, John Helfrich and other colleagues in the MIT Joint Program for valuable discussions and comments. Ronald Prinn and Henry Jacoby provided us with Fig. 1 of this manuscript. We thank the reviewer for the insightful reviews and comments on earlier versions of the manuscript.

REFERENCES

Aber, J. D. 1992. Terrestrial ecosystems. In: K. E. Trenberth (ed.): *Climate system modeling.* Cambridge University Press, New York, 173–200.

Buol, S. W., P. A. Sanchez, J. M. Kimble and S. B. Weed. 1990. Predicted impact of climate warming on soil properties and use. In: B. A. Kimball et al. (eds.): *Impact of carbon dioxide, trace gases and climate change on global agriculture.* ASA Spec. Publ. **53**, 71–82.

Cramer, W. P. and R. Leemans. 1993. Assessing impacts of climate change on vegetation using climate classification systems. In: A. M. Solomon and H. H. Shugart (eds.): *Vegetation dynamics and global change.* Chapman & Hall. New York, 191–217.

Emanuel, W. R., H. H. Shugart and M. P. Stevenson. 1985. Climatic change and the broad-scale distribution of terrestrial ecosystem complexes. *Climatic Change* **7**, 29–43.

Esser, G. 1987. Sensitivity of global carbon pools and fluxes to human and potential climate impact. *Tellus* **39B**, 245–260.

Esser, G. 1990. Modeling global terrestrial sources and sinks of CO_2 with special reference to soil organic matter. In: A. F. Bouwman (ed.): *Soils and greenhouse effect.* John Wiley, New York, 247–262.

Eswaran, H., E. Van Der Berg and P. Reich. 1993. Organic carbon in soils of the world. *Soil Science Society of America Journal* **57**, 192–194.

FAO/CSRC/MBL. 1974. *Soil map of the world, 1:5,000,000.* Unesco, Paris, France. Digitization (0.5° resolution) by Complex Systems Research Center, University of New Hampshire, Durham and modifications by Marine Biological Laboratory, Woods Hole, USA.

Gates, D. M. 1985. Global biospheric response to increasing atmospheric carbon dioxide concentration. In: B. R. Strain and J. D. Cure (eds.): *Direct effect of increasing carbon dioxide on vegetation.* DOE/

ER-0238. United States Department of Energy,Washington, D. C., USA. p171–184.

Hahn, J., S. G. Warren, J. London and J. L. Roy. 1988. *Climatological data for clouds over the globe from surface observation.* United States Department of Energy, Oak Ridge, Tennessee, U.S.A.

Hansen, J., G. Russel, D. Rind, P. Stone, A. Lacis, S. Lebedeff, R. Ruedy and L. Travis. 1983. Efficient three dimensional global models for climate studies: Model I and II. *Mon. Wea. Rev.* **111**, 609–662

Hansen, J., A. Lacis, D. Rind, G. Russel, P. Stone, I. Fung, R. Ruedy and J. Lerner. 1984. Climate sensitivity: Analysis of feedback mechanisms. In: J. E. Hansen and T. Takahashi (eds.): Climate process and Climate Sensitivity, *Geophysical Monograph* **29**, Maurice Ewing series 5, American Geophysical Union, Washington, D. C., 130–163.

Houghton, R. A. and G. M. Woodwell. 1989. Global climatic change. *Scientific American* **260**, 36–47.

Idso, S. B. and B. A. Kimball. 1993. Tree growth in carbon dioxide enriched air and its implications for global carbon cycling and maximum levels of atmospheric CO_2. *Global Biogeochemical Cycles* **8**, 537–555.

Idso, K. E. and S. B. Idso. 1994. Plant responses to atmospheric CO_2 enrichment in the face of environmental constraints: a review of the last 10 years' research. *Agricultural and Forest Meteorology* **69**, 153–203.

IPCC Working Group II. 1996. *Climate change 1995: scientific-technical analysis of impacts, adaptations and mitigation of climate change.* Intergovernmental Panel on Climate Change. Cambridge University Press. New York, p19

IPCC. 1995. *Climate Change 1994: Radiative forcing of climate change and an evaluation of the IPCC IS92 emission scenarios.* Intergovernmental Panel on Climate Change. Cambridge University Press. New York, 196–197.

IPCC. 1994. IPCC WGI report: *Radiative forcing of climate change.* Intergovernmental Panel on Climate Change. WMO/UNEP, Geneva. p5.

Jacoby, H. D. and R. G. Prinn. 1994. *Uncertainty in climate change policy analysis.* MIT Joint Program on the Science and Policy of Global Change Report 1. Massachusetts Institute of Technology, 34pp.

Jenkinson, D. S., D. E. Adams and A. Wild. 1991. Model estimate of CO_2 emissions from soil in response to global warming. *Nature* **351**, 304–306.

Kimball, B. A. 1975. Carbon dioxide and agricultural yield: an assemblage and analysis of 430 prior observations. *Agronomy Journal* **75**, 779–788.

Leemans, R. and W. P. Cramer. 1991. *The IIASA climate database for land areas on a grid with 0.5° resolution.* Research Report RR-91–18, International Institute for Applied Systems Analysis (IIASA), Laxenburg, Austria. 60pp.

Legates, D. R. and C. J. Willmott. 1988. *Global air temperature and precipitation data archive.* Department of Geography, University of Delaware, Newark, Delaware, U.S.A.

Manabe, S. and R. T. Wetherald. 1987. Large scale changes in soil wetness induced by an increase in carbon dioxide. *Journal of the Atmospheric Sciences* **44**, 1211–1235.

McGuire, A. D., J. M. Melillo, D. W. Kicklighter and L. A. Joyce. 1995. Equilibrium responses of soil carbon to climate change: empirical and process-based estimates. *J. of Biogeography* **22**, 785–796.

McGuire, A. D., L. A. Joyce, D. W. Kicklighter, J. M. Melillo, G. Esser and C. J. Vorosmarty. 1993.Productivity response of climax temperate forests to elevated temperature and carbon dioxide: a North America comparison between two global models. *Climatic Change* **24**, 287–310.

McGuire, A. D., J. M. Melillo, L. A. Joyce, D. W. Kicklighter, A. L. Grace, B. Moore III and C. J. Vorosmarty. 1992. Interactions between carbon and nitrogen dynamics in estimating net primary productivity for potential vegetation in North America. *Global Biogeochemical Cycles* **6**, 101–124.

Melillo, J. M. 1994. Modeling land-atmospheric interaction: A short review. In: W. B. Meyer and B. L. Turner (eds). *Changes in land use and land cover: a global perspective.* Cambridge University Press, 387–409.

Melillo, J. M., T. V. Callaghan, F. I. Woodward, E. Salati and S. K. Sinha. 1990. Climate change effects on ecosystems. In: J. T. Houghton, G. J. Jenkins and J. J. Ephraums (eds.): *Climatic change: The IPCC Scientific Assessment.* Cambridge University Press, New York. 282-310.

Melillo, J. M., A. D. McGuire, D. W. Kicklighter, B. Moore III, C. J. Vorosmarty and A. L. Schloss. 1993. Global climate change and terrestrial net primary production. *Nature* **363**, 234–240.

Melillo, J. M., D. W. Kicklighter, A. D. McGuire, W. T. Peterjohn and K. M. Newkirk. 1995. Global change and its effects on soil organic carbon stocks. In: R. G. Zepp and Ch. Sonntag (eds.): *Rôle of nonliving organic matter in the earth's carbon cycle.* John Wiley and Sons Ltd, 175–189.

NCAR/NAVY. 1984. *Global 10-minute elevation data.* Digital tape available through National Oceanic and Atmospheric Administration, National Geophysical Data Center, Boulder.

OECD. 1992. *The economic costs of reducing CO_2 emissions.* OECD Economic Studies No.19 OECD, Paris, France, 209pp.

Owensby, C. E., P. I. Coyne, J. M. Ham, L. M. Auen and A. K. Knapp. 1993. Biomass production in a tallgrass prairie ecosystem exposed to ambient and elevated CO_2. *Ecological Applications* **3**, 644–653.

Pan, Y., A. D. McGuire, D. W. Kicklighter and J. M. Melillo. 1996. The importance of climate and soils for estimates of net primary production: A sensitivity analysis with the Terrestrial Ecosystem Model. *Global Change Biology* **2**, 5–23.

Parton, W. J., J. M. O. Scurlock, D. S. Ojima, D. S. Schimel, D. O. Hall and SCOPE GRAM group members. 1995. Impact of climate change on grassland production and soil carbon worldwide. *Global Change Biology* **1**, 13–22.

Polley, H. W., H. B. Johnson, B. D. Marino and H. S. Mayeux. 1993. Increase in C_3 plant water use efficiency and biomass over Glacial to present CO_2 concentrations. *Nature* **361**, 61–63.

Post, W. M., W. R. Emanuel, P. J. Zinke and A. G. Stangenberger. 1982, Soil carbon pools and world life zones. *Nature* **298**, 156–159.

Potter, C. S., J. T. Randerson, C. B. Field, P. A. Matson, P. M. Vitousek, H. A. Mooney and S. A. Klooster. 1993. Terrestrial ecosystem production: a process model based on global satellite and surface data. *Global Biogeochemical Cycles* **7**, 811–841.

Raich, J. W., E. B. Rastetter, J. M. Melillo, D. W. Kicklighter, P. A. Steudler, B. J. Peterson, A. L. Grace, B. Moore III and C. J. Vorosmarty. 1991. Potential net primary productivity in south America: application of a global model. *Ecological Applications* **1**, 399–429.

Rind, D., R. Healy, C. Parkinson and D. Martinson. 1995. The role of sea ice in $2 \times CO_2$ climate model sensitivity. Part I: The total influence of sea ice thickness and extent. *Journal of Climate* **8**, 449–463.

Rosenzweig, C. and M. L. Parry. 1994. Potential impact of climate change on world food supply. *Nature* **367**, 133–138.

Russell, G. L., J. R. Miller and L. -C. Tsang 1985: Seasonal ocean heat transport computed from an atmospheric model. *Dyn. Atmos. Oceans*, **9**, 253–271.

Schimel, D. S., B. H. Braswell, E. A. Holland, R. McKeown, D. S. Ojima, T. H. Painter, W. J. Parton and A. R. Townsend. 1994. Climatic, edaphic and biotic controls over storage and turnover of carbon in soils. *Global Biogeochemical Cycles* **8**, 279–293.

Schlesinger, M. E. and Z. Zhao. 1989. Seasonal climatic changes induced by doubled CO2 as simulated by the OSU atmospheric GCM/mixed-layer ocean model. *J. of Climate* **2**, 459–495.

Schlesinger, W. H. 1977. Carbon balance in terrestrial detritus. *Annual Review of Ecology and Systematic* **8**, 51–81.

Sokolov, A. P. and P. H. Stone, 1994. Climate feedbacks study: results of numerical experiments with 2-dimensional statistical-dynamical model. Abstracts of the AGU 1994 Fall Meeting, *Eos.*

Sokolov, A. P. and P. H. Stone. 1995. *Description and validation of the MIT version of the GISS 2-D model.* MIT Joint Program on the Science and Policy of Global Change Report 2. Massachusetts Institute of Technology, 46pp.

Stone, P. H. and M. S. Yao. 1987. Development of a two-dimensional zonally averaged statistical-dynamical model. Part II. The role of eddy momentum fluxes in the general circulation and their parameterization. *J. Atmos. Sci.* **44**, 3769–3786.

Stone, P. H. and M. S. Yao. 1990. Development of a two-dimensional zonally averaged statistical-dynamical model. Part III. The parameterization of the eddy fluxes of heat and moisture. *J. of Climate* **3**, 726–740.

VEMAP Members. 1995. Vegetation/ecosystem modeling and analysis project (VEMAP): comparing biogeography and biogeochemistry models in a continental-scale study of terrestrial ecosystem responses to climate change and CO_2 doubling. *Global Biogeochemical Cycles* **9**, 407–437.

Vorosmarty, C. J., B. Moore III, A. L. Grace, M. P. Gildea, J. M. Melillo, B. J. Peterson, E. B. Rastetter and P. A. Steudler. 1989. Continental scale models of water balance and fluvial transport: an application to South America. *Global Biogeochemical Cycle* **3**, 241–265

Wetherald, R. T. and S. Manabe. 1988. Cloud feedback processes in a general circulation model. *J. Atmos. Sci.* **45**, 1397–1415.

Whittaker, R. H. and G. E. Likens. 1973. Primary production: The biosphere and man. *Human Ecology* **1**, 357–369.

Willmott, C. J., M. R. Clinton and W. D. Philpot. 1985. Small-scale climate maps: a sensitivity analysis of some common assumptions associated with grid-point interpolation and contouring. *The American Cartographer* **12**, 5–16.

Wilson, C. A. and J. F. B. Mitchell. 1987. A doubled CO_2 climate sensitivity experiment with a global climate model including a simple ocean. *J. of Geophysical Research* **92**, 13315–13343.

Woodward, F. I. and I. F. KcKee. 1991. Vegetation and climate. *Environment International* **17**, 535–546.

Yao, M. S. and P. H. Stone. 1987. Development of a two-dimensional zonally averaged statistical-dynamical model. Part I: The parameterization of Moist convection and its role in the general circulation. *J. Atmos. Sci.* **44**, 65–82.

Zhang, Xinshi. 1993. A vegetation-climate classification system for global change studies in China. *Quaternary Sciences* **2**, 157–169 (in Chinese with English abstract)